Published for SISSA by Springer

Received: November 22, 2016
Accepted: January 6, 2017
Published: January 17, 2017

JHEP01(2017)073

On top quark mass effects to gg → ZH at NLO

Alexander Hasselhuhn, Thomas Luthe and Matthias Steinhauser

Institut für Theoretische Teilchenphysik, Karlsruhe Institute of Technology (KIT), Wolfgang-Gaede Straße 1, Karlsruhe, D-76128 Germany

E-mail: alexander.hasselhuhn@udo.edu, thomas.luthe@kit.edu, matthias.steinhauser@kit.edu

Abstract: We compute next-to-leading order QCD corrections to the process $gg \to ZH$. In the effective-theory approach we confirm the results in the literature. We consider top quark mass corrections via an asymptotic expansion and show that there is a good convergence below the top quark threshold which describes approximately a quarter of the total cross section. Our corrections are implemented in the publicly available C++ program ggzh.

Keywords: NLO Computations, QCD Phenomenology

ArXiv ePrint: 1611.05881

doi:10.1007/JHEP01(2017)073

Contents

1 Introduction

In the upcoming years the general purpose experiments ATLAS and CMS at the CERN LHC will collect a large amount of data which will be used to perform precision studies of various quantities. Among them are certainly the properties of the Higgs boson, in particular its couplings to the other particles of the Standard Model. Important quantities in this context are the production cross sections and partial decay rates of the Higgs boson. The dominant production process is via gluon fusion followed by vector boson fusion and the so-called Higgs-strahlung process $pp \to VH$ ($V = Z, W$) which is the subject of the current paper. Although $pp \to VH$ has a much smaller cross section it is a promising channel to observe, e.g., if the Higgs boson decays to a $b\bar{b}$ pair once substructure techniques are applied [1].

The leading order (LO) cross section is obtained from the Drell-Yan process for the production of a virtual gauge boson $V^\star$ and its subsequent decay into VH. Next-to-next-to-leading order QCD corrections to this channel have been computed in refs. [2–6] and electroweak corrections have been considered in refs. [7, 8]. QCD corrections up to NNLO and electroweak corrections up to NLO for the total cross section have been implemented in the program `vh@nnlo` [9].

In ref. [10] the loop-induced production channel $gg \to ZH$ has been computed at leading order. NLO QCD corrections have been computed in ref. [11] in the heavy top quark limit which significantly simplifies the calculation. They are also implemented in `vh@nnlo` [9]. Note that the NLO corrections to $gg \to ZH$ are formally N^{3}LO contributions to $pp \to ZH$. However, due to the numerical importance of the gluon-induced process it is worthwhile to compute $gg \to ZH$ to NLO accuracy.

In this paper we study the effect of a finite top quark mass. At LO exact results are available. However, at NLO the occurring integrals are highly nontrivial and their

JHEP01(2017)073

evaluation is beyond straightforward application of current multi-loop techniques. We investigate the mass effects by expanding the amplitudes for large m_t. This approximation is not valid in all phase space regions. However, it provides an estimate of the numerical size of the power-suppressed terms and thus of the quality of the effective-theory result. Furthermore, it constitutes an important reference for a future exact result since we observe a good convergence of the partonic cross sections below the top quark pair threshold. We only consider the gg channel; similar techniques can also be applied to the loop-induced contributions of the qg and $q\bar{q}$ channels which are, however, numerically much smaller [11]. In our calculation we do not consider decays of the final-state Z boson.

Similar to $gg \to ZH$ also the process $gg \to HH$ is mediated by heavy quark loops. NLO and NNLO corrections have been considered in a series of papers [12–21] applying various approximations. Recently the exact NLO corrections became available [22, 23]. The comparison to the approximations shows sizeable differences for the total cross section and the Higgs transverse momentum distribution. However, reasonable agreement between the exact and the in $1/m_t$-expanded results is found for the Higgs pair invariant mass (m_{HH}) distribution for not too large values of m_{HH} if the approximated result is re-scaled with the exact LO cross section. Note that the region between the production threshold and the top quark threshold corresponds to about 100 GeV in the case of HH and to about 135 GeV in the case of ZH production which makes the heavy-top expansion more interesting for the latter.

Top quark mass effects have also been computed for the related process $gg \to ZZ$. In ref. [24] $1/m_t^2$ corrections have been computed at NLO, and interference effects have been considered in [25]. In the latter reference Padé approximation and conformal mapping has been applied to improve the validity of the expansion in $1/m_t$.

The remainder of the paper is organized as follows: in section 2 we briefly discuss the LO cross section and compare the in $1/m_t$ expanded and exact results. In section 3 we present our findings for the partonic NLO cross section. In particular, we identify the approximation procedure which leads to promising hadronic results, subject of section 4. We summarize our results in section 5.

2 $gg \to ZH$ at LO

Sample Feynman diagrams contributing to the LO cross section are shown in figure 1a and 1b. There are triangle contributions where the final-state Z and Higgs bosons are produced via a s-channel Z or Goldstone boson exchange. Both bottom and top quarks can be present in the loop. In the case of the box diagrams the Higgs boson couples directly to the quark running in the loop and thus only internal top quarks are present since we neglect the bottom Yukawa coupling. The effect of a finite bottom quark mass on the LO cross section is at the per mille level.

In the heavy-m_t approximation the diagrams with internal top quarks reduce to vacuum integrals. The massless triangle diagrams are computed with the help of simple form factor-type integrals which can be expressed in terms on Γ functions (see, e.g., appendix A of ref. [26]).

JHEP01(2017)073

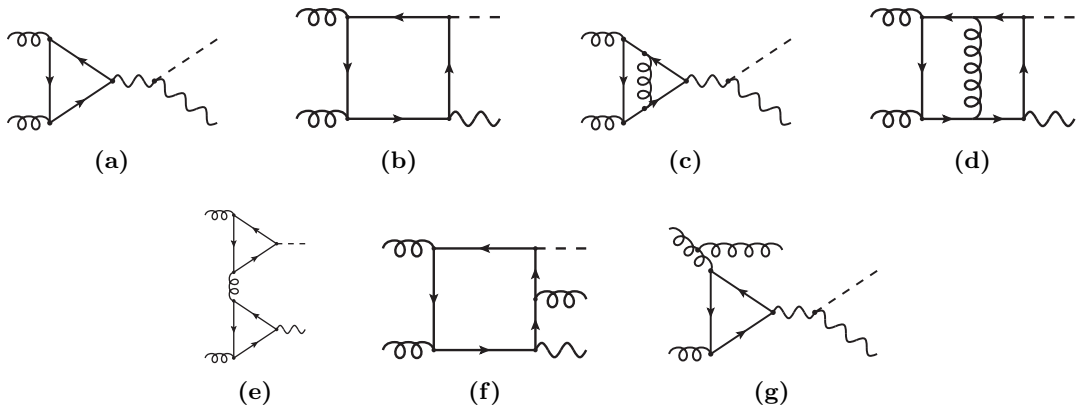

Figure 1. Sample Feynman diagram contributing to $gg \to ZH$ at LO and NLO. Solid, wavy, dashed and curly lines denote quarks, Z and Higgs bosons, and gluons, respectively. Internal wavy lines can also represent Goldstone bosons.

We perform the calculation for general R_ξ gauge and check that the gauge parameter ξ_Z present in the Z and Goldstone boson propagators drops out in the result for the cross section. In fact, it cancels between the diagrams with top and bottom quark triangles and a neutral Goldstone boson or a Z boson in the s channel. Note, that for special choices of ξ_Z the calculation can be significantly simplified. For example, in Landau gauge the massless triangle contribution with virtual Z boson vanishes [11]. Note that due to Furry's theorem there is no contribution from the vector coupling of the Z. Altogether there are 16 LO Feynman diagrams, all of them are individually finite.

We compute the LO amplitudes both in an expansion for large top quark mass including terms up to order $1/m_t^8$, and without applying any approximation and keeping the full top quark mass dependence. In the latter case we have reduced the tensor integrals to scalar three- and four-point integrals which are evaluated using the `LoopTools` library [27, 28]. We want to mention that in the limit $m_t \to \infty$ the calculation is significantly simplified. In particular, all top quark triangle contributions with a coupling of the Z boson vanish.

For the numerical results we use the following input values [29]

$$\begin{aligned} M_Z &= 91.1876\,\text{GeV}\,, \\ M_W &= 80.385\,\text{GeV}\,, \\ M_H &= 125\,\text{GeV}\,, \\ G_\mu &= 1.16637 \cdot 10^{-5}\,\text{GeV}^{-2}\,, \\ M_t &= 173.21\,\text{GeV}\,, \end{aligned} \tag{2.1}$$

where M_t is the top quark pole mass. To obtain our numerical results we follow ref. [11] and use the so-called G_μ scheme where the electromagnetic coupling constant α and the weak mixing angle ($s_W \equiv \sin\theta_W$) are defined via

$$\begin{aligned} c_W^2 &= 1 - s_W^2 \;=\; \frac{M_W^2}{M_Z^2} \;\approx\; 0.77710\,, \\ \alpha &= \frac{\sqrt{2} G_\mu M_W^2 s_W^2}{\pi} \;\approx\; 0.0075623\,. \end{aligned} \tag{2.2}$$

JHEP01(2017)073

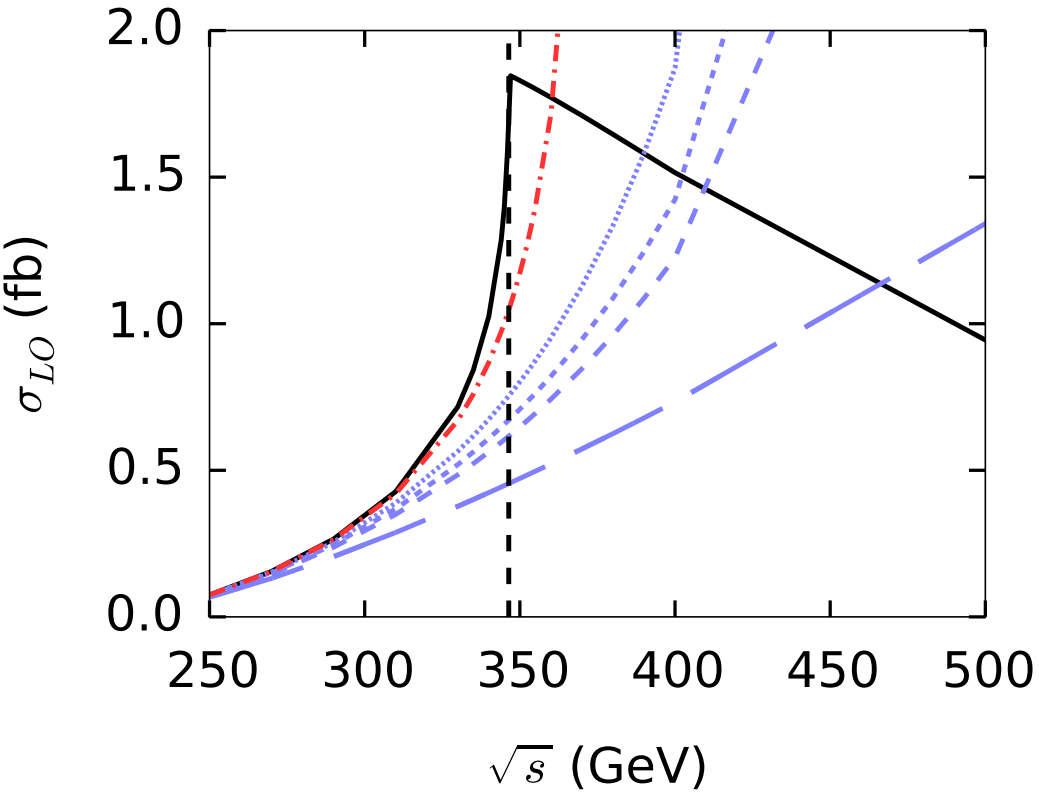

Figure 2. LO $gg \to ZH$ partonic cross section as a function of the partonic center-of-mass energy $\sqrt{s}$. The exact result is shown as black solid line and the expansion terms including $1/m_t^0, \ldots, 1/m_t^8$ terms (note that the $1/m_t^2$ term vanishes) are represented by (blue) dashed lines where shorter-dashed lines include higher order power corrections. The dash-dotted (red) line represents the [2/2]-Padé result, see text.

Our default PDF set is `PDF4LHC15_nlo_100_pdfas` [30] which we use to compute both the LO and NLO cross sections. For the strong coupling constant we use the value provided by `PDF4LHC15_nlo_100_pdfas` which is given by

$$\alpha_s(M_Z) = 0.118\,. \tag{2.3}$$

For the implementation of the PDFs we use version 6.1.6 of the `LHAPDF` library [31] (see https://lhapdf.hepforge.org/) which also provides the running for α_s form M_Z to the chosen renormalization scale μ_R. Our default choice for the latter and for the factorization scale μ_F is the invariant mass of the ZH system

$$\mu_0^2 = (p_H + p_Z)^2\,. \tag{2.4}$$

If not stated otherwise we choose $s_H = 14\,\text{TeV}$ for the hadronic center-of-mass energy.

In figure 2 we compare the partonic cross section of the exact (black solid line) and expanded results (blue dashed lines, see caption for details). One observes a continuous improvement of the large-m_t approximations below the top quark pair threshold which is at $\sqrt{s} \approx 346\,\text{GeV}$. However, the characteristic behaviour at threshold and the drop of

JHEP01(2017)073

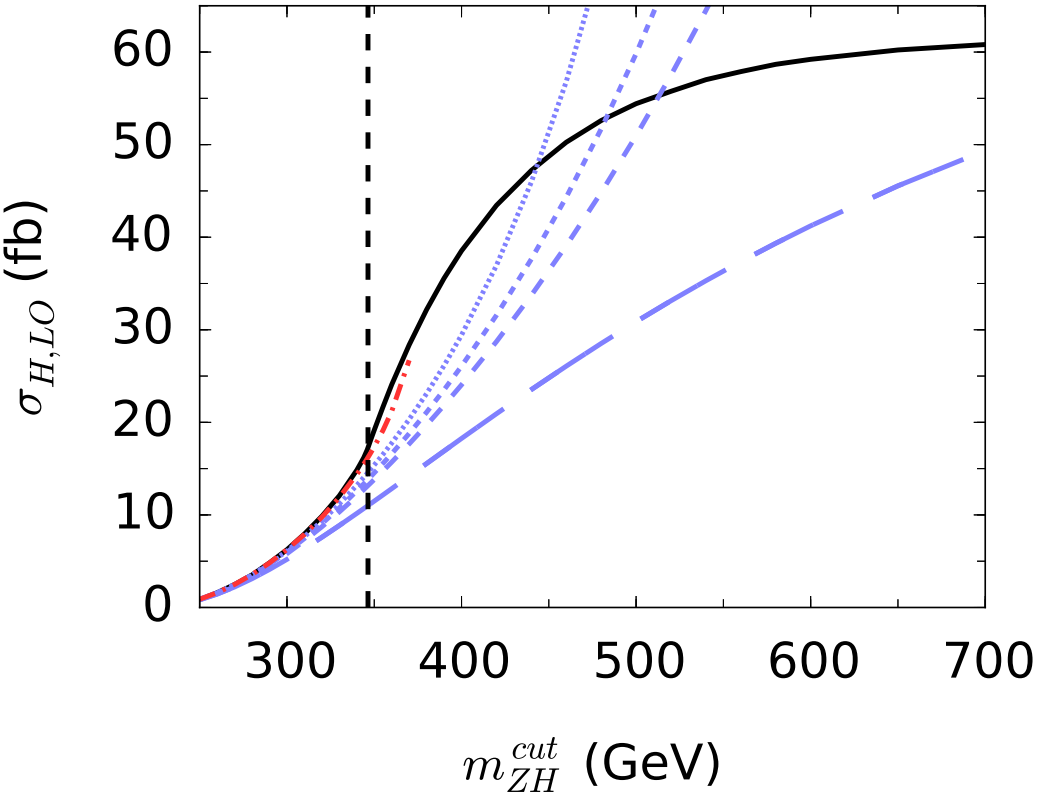

Figure 3. Hadronic LO $gg \to ZH$ cross section as a function of $m_{ZH}^{\rm cut}$, the cut on the invariant mass of the Z-Higgs system. The exact result is shown in black. The dashed (blue) curves correspond to the expanded results (see caption of figure 2 for more details) and the [2/2]-Padé approximation is shown as dash-dotted (red) curve.

the cross section for large values of $\sqrt{s}$ cannot be reproduced. We pick up the idea of ref. [25][1] and use the expansion terms to construct the [2/2]-Padé approximant, see (red) dash-dotted line in figure 2. One observes that the Padé result approximates reasonably well the exact curve up to $\sqrt{s} \approx 346\,\text{GeV}$ which is indicated by the vertical dashed line.

In figure 3 we show the hadronic cross section for $gg \to ZH$ as a function of the cut on the invariant mass of the Z-Higgs system using the same conventions as in figure 2. We observe a rapid convergence of the $1/m_t$ expansion (blue dashed curves) for $m_{ZH}^{\rm cut} \lesssim 350\,\text{GeV}$ and a good approximation of the exact result (solid, black) by the Padé curve (dash-dotted, red). By construction, for large values of $m_{ZH}^{\rm cut}$ the total cross section is reproduced. It is interesting to note that for $m_{ZH}^{\rm cut} \lesssim 346\,\text{GeV}$ the cross section amounts to about a quarter of total cross section. For this value of $m_{ZH}^{\rm cut}$ the Padé result yields 16.1 fb which is very close to the exact result (17.0 fb). On the other hand, the infinite top mass approach only gives 11.0 fb.

For a collision energy of $\sqrt{s_H} = 8\,\text{TeV}$ we obtain for the total hadronic cross section $\sigma_{\rm H,LO}^{\rm (exact)} = 16.0\,\text{fb}$ which agrees impressively well with the result obtained from the effective-

[1] In contrast to [25] we apply the Padé approximation at the level of differential cross sections and not at the level of the amplitudes. Furthermore, we refrain from performing a conformal mapping since in our case the gain is marginal.

JHEP01(2017)073

theory approximation: 15.8 fb. Since the partonic cross sections have completely different shapes (cf. solid and long-dashed curves in figure 2) this agreement has to be considered as accidental. In fact, for $\sqrt{s_H} = 14\,\text{TeV}$ we have $\sigma^{(\text{exact})}_{\text{H,LO}} = 61.8\,\text{fb}$ whereas the infinite-m_t approximation gives 80.5 fb.

3 Partonic NLO corrections

Sample Feynman diagrams contributing to the real and virtual NLO corrections can be found in figure 1. In our calculation we apply standard techniques. In particular, the one- and two-loop integrals are reduced to master integrals using the program `FIRE` [32]; the resulting master integrals can be found in refs. [33, 34]. For the isolation of the soft and collinear infrared divergences we follow ref. [35] which allows to compute differential cross sections. Although we consider top quark mass effects we express our final result in terms of α_s defined in the five-flavour theory.

We write the partonic cross section to NLO accuracy in the form

$$\sigma_{\text{NLO}} = \sigma^{(\text{exact})}_{\text{LO}} + \delta\sigma^{(\text{approx})}_{\text{NLO}} + \delta\sigma^{(\text{virt,red})}_{\text{NLO}}\,, \tag{3.1}$$

where results for the LO cross section have already been discussed in section 2.

$\delta\sigma^{(\text{virt,red})}_{\text{NLO}}$ is the contribution from the reducible diagrams where two quark triangles are connected by a gluon in the t or u channel, see figure 1e for a sample Feynman diagram. In ref. [11] the effective-theory result for the corresponding differential cross section is given, which is obtained by considering the interference with the LO amplitude. We confirm the analytic expression of [11] and add power-suppressed terms up to order $1/m_t^8$. Furthermore, we have computed this contribution exactly keeping the full top mass dependence. For the numerical results which we present in section 4 the exact expression is used.

In this section we discuss $\delta\sigma^{(\text{approx})}_{\text{NLO}}$. We define the NLO approximation by factoring out the exact LO cross section multiplied by the ratio of the in $1/m_t$ expanded NLO and LO contribution:

$$\delta\sigma^{(\text{approx})}_{\text{NLO}} = \sigma^{(\text{exact})}_{\text{LO}}\,\frac{\delta\sigma^{(\text{exp-}n)}_{\text{NLO}}}{\sigma^{(\text{exp-}n)}_{\text{LO}}}\,, \tag{3.2}$$

where "exp-n" means that the corresponding quantity contains expansion terms up to order $1/m_t^n$.

In figure 4 we show as (blue) dashed lines the quantities $\delta\sigma^{(\text{exp-}n)}_{\text{NLO}}$ and as (red) dashed-dotted line the [2/2]-Padé approximant as a function of the partonic center-of-mass energy $\sqrt{s}$. We observe a similar behaviour as at LO (cf. figure 2). In particular, it can not be expected that meaningful NLO approximations are obtained for large values of $\sqrt{s}$ from these expansion terms. However, based on observations at LO we expect that the Padé result provides a reasonable approximation below $\sqrt{s} \approx 346\,\text{GeV}$. In figure 4 we also show as (yellow) long- and short-dashed curves the quantity $\delta\sigma^{(\text{approx})}_{\text{NLO}}$ with $n = 0$ and 8 (the curves for $n = 2, 4, 6$ lie in between and are not shown for clarity). The shape is now dictated by the LO cross section and has a well-behaved high-energy limit. For $\sqrt{s} < 346\,\text{GeV}$ the two

JHEP01(2017)073

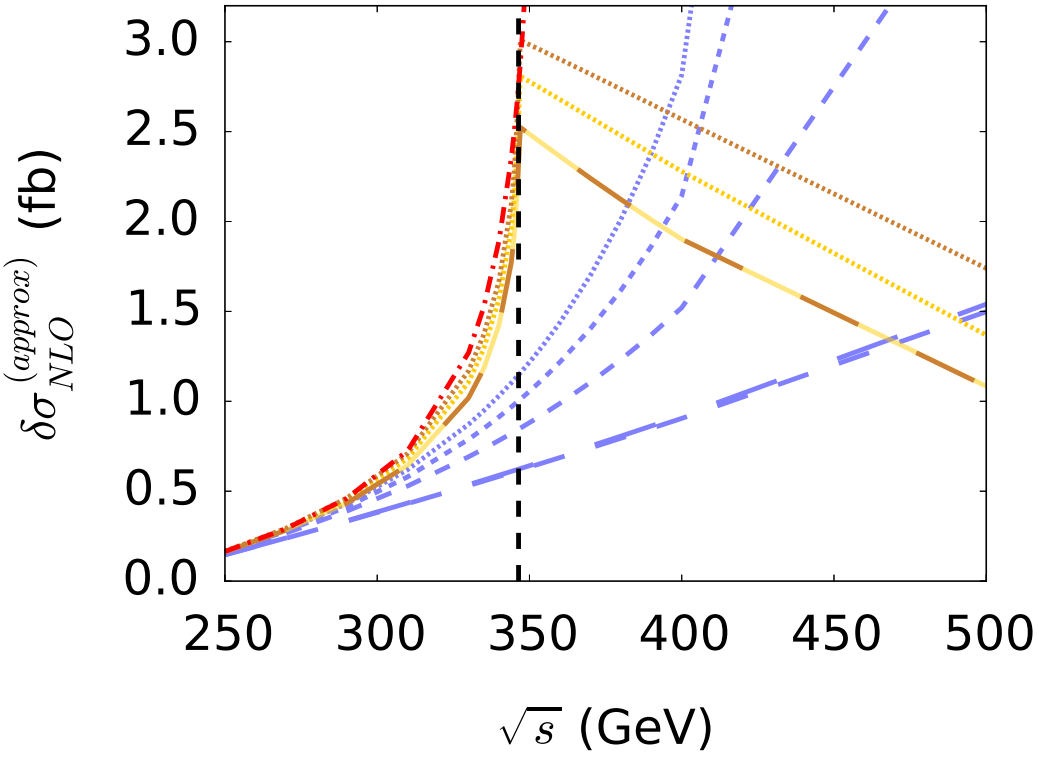

Figure 4. NLO partonic cross section as a function of $\sqrt{s}$. The expansion terms including $1/m_t^0, \ldots, 1/m_t^8$ terms are represented by (blue) dashed lines where shorter-dashed lines include higher order power corrections. The dash-dotted (red) line represents the [2/2]-Padé result. Approximations based on eqs. (3.2) and (3.3) are shown as yellow and brown curves, respectively. In both cases we either include only the leading top quark mass corrections (long-dashed curves) or corrections up to order $1/m_t^8$ (short-dashed curves).

curves are close together, however above the top threshold the $n = 8$ curve is significantly higher.

As an alternative to eq. (3.2) we consider an approach where the exact LO result is factored at the differential level, i.e., before the integration over phase space. Schematically we write

$$\int \mathrm{dPS}_2 \left|\mathcal{M}_{\mathrm{LO}}^{(\mathrm{exact})}\right|^2 \frac{\left|\mathcal{M}_{\mathrm{NLO}}^{(\text{exp-n})}\right|^2}{\left|\mathcal{M}_{\mathrm{LO}}^{(\text{exp-n})}\right|^2}\,, \tag{3.3}$$

where "dPS_2" indicates that we use this kind of factorization for the two-particle phase space contributions. The contribution from the three-particle phase space (which is numerically small) is added in the infinite top quark mass approximation. The integrand of eq. (3.3) is better behaved than the one for $\delta\sigma_{\mathrm{NLO}}^{(\text{exp-}n)}$ in eq. (3.2), which might lead to better approximations for the total cross section. However, below the top quark pair threshold we only expect small differences between eqs. (3.2) and (3.3).

Figure 4 shows $\delta\sigma_{\mathrm{NLO}}^{(\mathrm{approx})}$ as obtained from eq. (3.3) for $n = 0$ and 8 as brown dashed lines. Note that the $n = 0$ curve lies almost on top of the yellow curve (which is based

JHEP01(2017)073

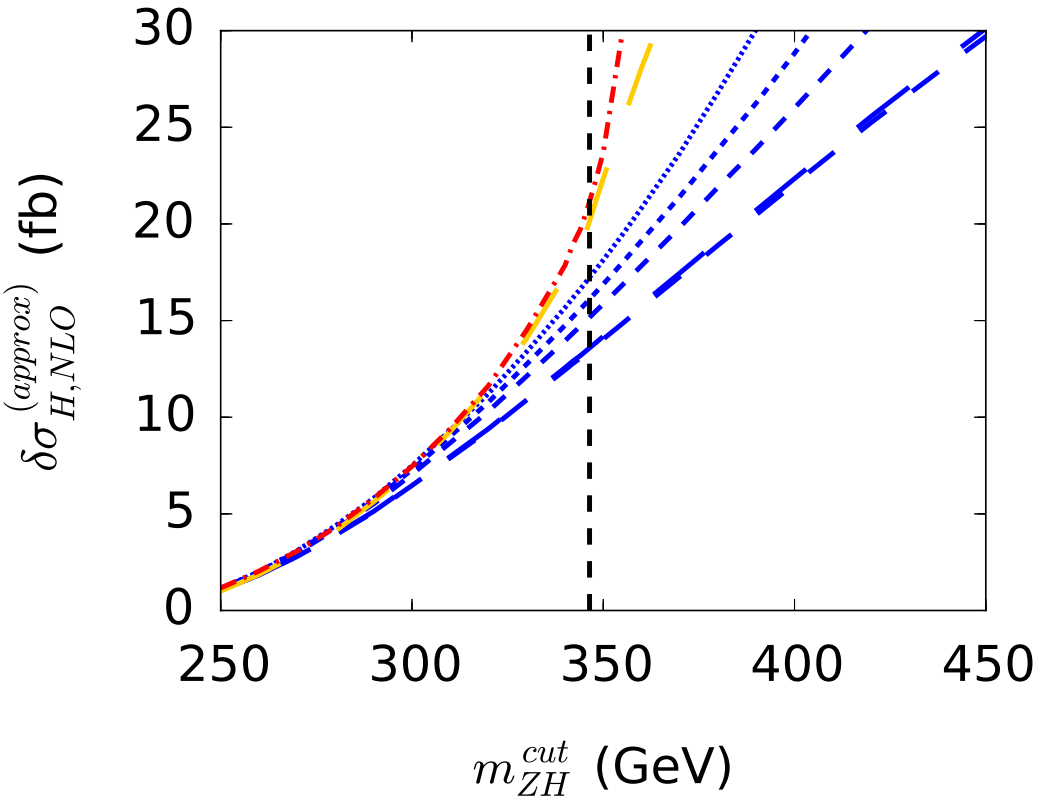

Figure 5. NLO contribution $\delta\sigma^{(\text{approx})}_{\text{H,NLO}}$ to the hadronic cross section as a function of m^{cut}_{ZH}. The dashed (blue) curves contain expansion terms up to order $1/m_t^8$ and the dash-dotted (red) curve represents the Padé result. The long-dashed (yellow) curve is based on eq. (3.2) with $n = 0$.

on eq. (3.2)). This is because the two-particle phase space contributions to the squared matrix elements are proportional to the LO result. Moreover the three-particle contribution is small. As before, the $n = 0$ and $n = 8$ curves are close together below the top threshold and significant deviations are observed above.

4 Numerical results for hadronic cross sections

Numerical results for the LO cross section have already been discussed in section 2. At NLO we write in analogy to eq. (3.1)

$$\sigma_{\text{H,NLO}} = \sigma^{(\text{exact})}_{\text{H,LO}} + \delta\sigma^{(\text{approx})}_{\text{H,NLO}} + \delta\sigma^{(\text{virt,red})}_{\text{H,NLO}} \,. \tag{4.1}$$

For the construction of $\delta\sigma^{(\text{approx})}_{\text{H,NLO}}$ we consider three possibilities: (i) we either use the in $1/m_t$ expanded partonic results; (ii) we construct an approximation using eq. (3.2) (where the partonic cross sections are replaced by their hadronic counterparts), or (iii) we utilize the differential approach of eq. (3.3). The latter option is only applied to the total cross section.

Figure 5 shows the m^{cut}_{ZH} dependence of the NLO contribution $\delta\sigma^{(\text{approx})}_{\text{H,NLO}}$. We concentrate on the region below the top quark threshold where approximations are valid. For large

JHEP01(2017)073

$\sqrt{s_H}$/GeV	$\sigma^{(\text{exact})}_{\text{H,LO}}$	$\sigma^{(\text{exp-0})}_{\text{H,NLO}}$	$\sigma^{(\text{re-scale})}_{\text{H,NLO}}$	$\sigma^{(\text{diff})}_{\text{H,NLO}}$	$\sigma^{[2/2]}_{\text{H,NLO}}$	NLO scale variation
7	11.2	23.9	24.9	26.1	26.5	$^{+21\%}_{-21\%}$
8	16.0	35.2	35.4	37.2	38.8	$^{+20\%}_{-20\%}$
13	52.4	129	113	121	140	$^{+14\%}_{-17\%}$
14	61.8	155	133	142	168	$^{+13\%}_{-16\%}$

Table 1. LO and NLO results for the total cross section in fb. In columns 3 to 6 the following NLO contributions are added to the exact LO result: infinite top mass approximation ($\sigma^{(\text{exp-0})}_{\text{H,NLO}}$), re-scaled NLO contribution based on eq. (3.2) ($\sigma^{(\text{re-scale})}_{\text{H,NLO}}$), re-scaled NLO contribution based on eq. (3.3) ($\sigma^{(\text{diff})}_{\text{H,NLO}}$), and the approximation where below the top threshold the [2/2]-Padé result and above the infinite top mass approximation is used ($\sigma^{[2/2]}_{\text{H,NLO}}$). The last column gives the scale uncertainties for $\sigma^{[2/2]}_{\text{H,NLO}}$ where $\mu_F = \mu_R$ is varied by $\mu_F/\mu_0 \in [1/3, 3]$. The NLO cross sections contain $\sigma^{(\text{virt,red})}_{\text{H,NLO}}$.

values of m^{cut}_{ZH} one obtains the total cross section which is briefly discussed below. The (blue) dashed curves are obtained from the asymptotically expanded results and the dash-dotted (red) curve is obtained from the [2/2]-Padé approximation. The general picture is similar to the one at partonic level. In particular, one observes a good convergence for $m^{\text{cut}}_{ZH} \lesssim 350\,\text{GeV}$ and one can expect that the Padé result provides a good approximation to the unknown exact result. Note that for $m^{\text{cut}}_{ZH} = 346\,\text{GeV}$ the large-m_t approximation gives 13 fb whereas the Padé result leads to 21 fb which corresponds to an increase of more than 50%. The total cross section for $m^{\text{cut}}_{ZH} = 346\,\text{GeV}$ amounts to about a quarter of the total cross section computed in the infinite top quark mass approximation (see also below).

The dashed yellow curve in figure 5 is based on eq. (3.2). It is obtained from the m^{cut}_{ZH}-dependence of the exact LO result multiplied by the ratio of the NLO and LO total cross sections taken in the infinite top quark mass approximation. Below $m^{\text{cut}}_{ZH} \lesssim 350\,\text{GeV}$ this result and the Padé curve lie basically on top of each other. Very similar results are also obtained if the ratio of the m^{cut}_{ZH}-dependent NLO and LO total cross sections are considered in the effective theory limit. For reasons of clarity the corresponding curve is not shown in figure 5.

We refrain from showing the m^{cut}_{ZH} dependence for $\delta\sigma^{(\text{virt,red})}_{\text{H,NLO}}$ since this contribution is numerically small. It is negative and amounts to about 1% of $\delta\sigma^{(\text{approx})}_{\text{NLO}}$. However, it is included in the discussion of the total cross section below. Although not visible in the plots we want to remark that the infinite top quark mass approximation of $\sigma^{(\text{virt,red})}_{\text{H,NLO}}$ is off by a factor two.

Table 1 shows the values for the total cross section at LO and for four possible approximations at NLO, see caption for details. Note, that in all NLO predictions finite top mass corrections are only considered for $\sqrt{s} < 346$ GeV. For higher values of s the infinite top mass limit is applied. The first three approximations treat the top quark as infinitely heavy, whereas the fourth one incorporates the heavy quark effects considered earlier in

JHEP01(2017)073

the form of a [2/2]-Padé approximation, which would be our recommendation for the best possible prediction to date. One observes, that the finite top mass corrections shift the total cross section upwards, however, the size is well within the scale uncertainties which are shown for $\sigma_{\mathrm{H,NLO}}^{[2/2]}$ in the last column. Similar uncertainties are also obtained for the other approximations.

The numerical results discussed in this section and in section 3 have been obtained with the help of the program `ggzh` which can be downloaded from [36]. A brief description of `ggzh` can be found in the appendix. `ggzh` can be used to reproduce the numerical results of ref. [11].

5 Conclusions

The associated production of a Higgs and Z boson is a promising channel in view of the determination of the Higgs boson couplings, in particular the Yukawa coupling to bottom quarks. We compute top quark mass effects to the loop-induced process $gg \to ZH$ at NLO in QCD by expanding the Feynman amplitudes in the limit of large top quark mass. Our leading term reproduces the results of ref. [11]. It is not expected that the top quark suppressed terms provide a good approximation for large partonic center-of-mass energies. However, we can show that below the production threshold of two top quarks, say for $\sqrt{s} \lesssim 350\,\mathrm{GeV}$, the $1/m_t$-expansion shows a good convergence at NLO. This is strongly supported by the good agreement of the re-scaled NLO approximation using the exact LO cross section and the [2/2]-Padé approximation constructed from expansion terms up to $1/m_t^8$. Thus, the corrections computed in this paper provide a good approximation to the m_{ZH} distributions below $\sqrt{s} \lesssim 350\,\mathrm{GeV}$. This region covers about 25% of the total cross section. Furthermore, the top mass corrections in this region constitute an important cross check once the exact calculation of the NLO corrections to $gg \to ZH$ is available. The numerical results presented in this work can be reproduced with the program `ggzh` which is publicly available from [36].

Acknowledgments

We are thankful to Kirill Melnikov for enlightening discussions and to Lorenzo Tancredi for providing analytic results for the amplitude $Z \to ggg$ from ref. [37] which we could compare to our results. We thank Robert Harlander for helping with the comparison to `vh@nnlo` [9]. This work is supported by the Deutsche Forschungsgemeinschaft through grant STE 945/2-1.

A Brief description of `ggzh`

Together with this paper we also publish the program `ggzh` which can be downloaded from [36]. `ggzh` includes all contributions to the process $gg \to ZH$ which are discussed in this paper.

JHEP01(2017)073

`ggzh` is written in `C++`. Before compilation it is necessary to install the libraries CUBA [38], `LoopTools` [27, 28] and `gsl` [39]. The corresponding paths should be inserted in the file `Makefile.local`. Afterwards, `make` starts the compilation.

The input file `xsection.cfg` defines the channels which shall be considered. Furthermore, one has to decide whether the partonic or hadronic cross section is considered, which pdf set is used and whether the sum of the considered channels is computed or not. Thus, `xsection.cfg` typically looks as follows

```
active channels: {LO_exact,LO_0}
pdf set: PDF4LHC15_nlo_100_pdfas
hadronic: true
sum channels: false
```

`ggzh` outputs partonic cross sections in case `hadronic: false` is chosen. In the sample file the exact LO cross section and the effective-theory result including $1/m_t^0$ terms is computed. Further available channels are `LO_<i>` with $i = 2, 4, 6, 8$ for the $1/m_t^i$ contribution and `pade22_LO` for the [2/2]-Padé approximation of the LO cross section. The $1/m_t^i$ contribution to $\delta\sigma_{\text{NLO}}^{(\text{approx})}$ is obtained by summing the channels `NLO_phase2_<i>`, `NLO_phase2eta_<i>` and `NLO_phase3_<i>` ($i = 0, 2, 4, 6, 8$) and $\delta\sigma_{\text{NLO}}^{(\text{virt,red})}$ is implemented in `NLO_reducible_exact`.

Results based on the differential factorization of eq. (3.3) can be obtained via the channels `NLO_differential_phase2` and `NLO_differential_phase2eta` (remember that eq. (3.3) is only applied to two-particle phase space contributions). The parameter `diff_order` in the input file `params.cfg` specifies the expansion depth used for the LO and NLO expressions in (3.3).

The second input file `params.cfg` contains the values for the various input parameters needed for the calculation. It overwrites the default values which are given in `params.def` together with a brief description of the meaning. The package comes with template files which clarify the syntax.

`ggzh` is launched by simply calling the executable in the shell

```
> ./ggzh
```

All input parameter are repeated in the output and the results for the individual channels is given in the form

```
Calculating hadronic cross-section for channel ``LO_exact''.
Integrating (Vegas) ...
Number of integrand evaluations: 1050000
Integration time: 49s. Per iteration: 0.04697ms
Result [1/(GeV)^2]: 1.5875696750976581e-10
Error  [1/(GeV)^2]: 7.5506640742330014e-13
Result [fbarn]:     61.816682911840118
Error  [fbarn]:     0.29400725786852289
Relative error:     0.0047561150812284996
```


JHEP01(2017)073

```
Chi^2 Probability:  0.18458145471778875
#points dropped:    0

Calculating hadronic cross-section for channel ``LO_0''.
Integrating (Vegas) ...
Number of integrand evaluations: 1050000
Integration time: 2s. Per iteration: 0.002444ms
Result [1/(GeV)^2]: 2.0665863953725464e-10
Error  [1/(GeV)^2]: 1.3007066760509459e-13
Result [fbarn]:     80.468604254996833
Error  [fbarn]:     0.050646830445289774
Relative error:     0.00062939864452967408
Chi^2 Probability:  6.004534622038346e-12
#points dropped:    0
```

Besides the total cross section it is also possible to introduce a cut on the invariant mass m_{ZH} which is switched on with `use_inv_mass_cutoff: 1` in the file `params.cfg`. The numerical values for the cut is specified with `inv_mass_cutoff: <m_ZH-value>`.

With the help of `use_mt_threshold: 1` one switches on the possibility to use the infinite top mass approximation above the value for $\sqrt{s}$ given by `mt_threshold: <mtthr-value>`.

`ggzh` contains the option to vary μ_R and μ_F independently. Furthermore, it is possible to choose fixed scales (e.g. $\mu_R = M_H$ or $\mu_R = m_t$) or identify the scales to the partonic center-of-mass energy.

References

[1] J.M. Butterworth, A.R. Davison, M. Rubin and G.P. Salam, *Jet substructure as a new Higgs search channel at the LHC*, *Phys. Rev. Lett.* **100** (2008) 242001 [arXiv:0802.2470] [INSPIRE].

[2] O. Brein, A. Djouadi and R. Harlander, *NNLO QCD corrections to the Higgs-strahlung processes at hadron colliders*, *Phys. Lett.* **B 579** (2004) 149 [hep-ph/0307206] [INSPIRE].

[3] O. Brein, R. Harlander, M. Wiesemann and T. Zirke, *Top-Quark Mediated Effects in Hadronic Higgs-Strahlung*, *Eur. Phys. J.* **C 72** (2012) 1868 [arXiv:1111.0761] [INSPIRE].

[4] G. Ferrera, M. Grazzini and F. Tramontano, *Associated WH production at hadron colliders: a fully exclusive QCD calculation at NNLO*, *Phys. Rev. Lett.* **107** (2011) 152003 [arXiv:1107.1164] [INSPIRE].

[5] G. Ferrera, M. Grazzini and F. Tramontano, *Higher-order QCD effects for associated WH production and decay at the LHC*, *JHEP* **04** (2014) 039 [arXiv:1312.1669] [INSPIRE].

JHEP01(2017)073

[6] G. Ferrera, M. Grazzini and F. Tramontano, *Associated ZH production at hadron colliders: the fully differential NNLO QCD calculation*, *Phys. Lett.* **B 740** (2015) 51 [arXiv:1407.4747] [INSPIRE].

[7] M.L. Ciccolini, S. Dittmaier and M. Krämer, *Electroweak radiative corrections to associated WH and ZH production at hadron colliders*, *Phys. Rev.* **D 68** (2003) 073003 [hep-ph/0306234] [INSPIRE].

[8] A. Denner, S. Dittmaier, S. Kallweit and A. Mück, *Electroweak corrections to Higgs-strahlung off W/Z bosons at the Tevatron and the LHC with HAWK*, *JHEP* **03** (2012) 075 [arXiv:1112.5142] [INSPIRE].

[9] O. Brein, R.V. Harlander and T.J.E. Zirke, *vh@nnlo — Higgs Strahlung at hadron colliders*, *Comput. Phys. Commun.* **184** (2013) 998 [arXiv:1210.5347] [INSPIRE].

[10] B.A. Kniehl, *Associated Production of Higgs and Z Bosons From Gluon Fusion in Hadron Collisions*, *Phys. Rev.* **D 42** (1990) 2253 [INSPIRE].

[11] L. Altenkamp, S. Dittmaier, R.V. Harlander, H. Rzehak and T.J.E. Zirke, *Gluon-induced Higgs-strahlung at next-to-leading order QCD*, *JHEP* **02** (2013) 078 [arXiv:1211.5015] [INSPIRE].

[12] S. Dawson, S. Dittmaier and M. Spira, *Neutral Higgs boson pair production at hadron colliders: QCD corrections*, *Phys. Rev.* **D 58** (1998) 115012 [hep-ph/9805244] [INSPIRE].

[13] J. Grigo, J. Hoff, K. Melnikov and M. Steinhauser, *On the Higgs boson pair production at the LHC*, *Nucl. Phys.* **B 875** (2013) 1 [arXiv:1305.7340] [INSPIRE].

[14] D. de Florian and J. Mazzitelli, *Higgs Boson Pair Production at Next-to-Next-to-Leading Order in QCD*, *Phys. Rev. Lett.* **111** (2013) 201801 [arXiv:1309.6594] [INSPIRE].

[15] D.Y. Shao, C.S. Li, H.T. Li and J. Wang, *Threshold resummation effects in Higgs boson pair production at the LHC*, *JHEP* **07** (2013) 169 [arXiv:1301.1245] [INSPIRE].

[16] F. Maltoni, E. Vryonidou and M. Zaro, *Top-quark mass effects in double and triple Higgs production in gluon-gluon fusion at NLO*, *JHEP* **11** (2014) 079 [arXiv:1408.6542] [INSPIRE].

[17] J. Grigo, K. Melnikov and M. Steinhauser, *Virtual corrections to Higgs boson pair production in the large top quark mass limit*, *Nucl. Phys.* **B 888** (2014) 17 [arXiv:1408.2422] [INSPIRE].

[18] J. Grigo, J. Hoff and M. Steinhauser, *Higgs boson pair production: top quark mass effects at NLO and NNLO*, *Nucl. Phys.* **B 900** (2015) 412 [arXiv:1508.00909] [INSPIRE].

[19] D. de Florian and J. Mazzitelli, *Higgs pair production at next-to-next-to-leading logarithmic accuracy at the LHC*, *JHEP* **09** (2015) 053 [arXiv:1505.07122] [INSPIRE].

[20] G. Degrassi, P.P. Giardino and R. Gröber, *On the two-loop virtual QCD corrections to Higgs boson pair production in the Standard Model*, *Eur. Phys. J.* **C 76** (2016) 411 [arXiv:1603.00385] [INSPIRE].

[21] D. de Florian et al., *Differential Higgs Boson Pair Production at Next-to-Next-to-Leading Order in QCD*, *JHEP* **09** (2016) 151 [arXiv:1606.09519] [INSPIRE].

[22] S. Borowka et al., *Higgs Boson Pair Production in Gluon Fusion at Next-to-Leading Order with Full Top-Quark Mass Dependence*, *Phys. Rev. Lett.* **117** (2016) 012001 [*Erratum ibid.* **117** (2016) 079901] [arXiv:1604.06447] [INSPIRE].

[23] S. Borowka et al., *Full top quark mass dependence in Higgs boson pair production at NLO*, *JHEP* **10** (2016) 107 [arXiv:1608.04798] [INSPIRE].

JHEP01(2017)073

[24] K. Melnikov and M. Dowling, *Production of two Z-bosons in gluon fusion in the heavy top quark approximation*, *Phys. Lett.* **B 744** (2015) 43 [arXiv:1503.01274] [INSPIRE].

[25] J.M. Campbell, R.K. Ellis, M. Czakon and S. Kirchner, *Two loop correction to interference in $gg \to ZZ$*, *JHEP* **08** (2016) 011 [arXiv:1605.01380] [INSPIRE].

[26] V.A. Smirnov, *Analytic Tools for Feynman Integrals*, *Springer Tracts Mod. Phys.* **250** (2012) 1 [INSPIRE].

[27] T. Hahn and M. Pérez-Victoria, *Automatized one loop calculations in four-dimensions and D-dimensions*, *Comput. Phys. Commun.* **118** (1999) 153 [hep-ph/9807565] [INSPIRE].

[28] G.J. van Oldenborgh and J.A.M. Vermaseren, *New Algorithms for One Loop Integrals*, *Z. Phys.* **C 46** (1990) 425 [INSPIRE].

[29] Particle Data Group collaboration, C. Patrignani et al., *Review of Particle Physics*, *Chin. Phys.* **C 40** (2016) 100001 [INSPIRE].

[30] J.M. Butterworth et al., *PDF4LHC recommendations for LHC Run II*, *J. Phys.* **G 43** (2016) 023001 [arXiv:1510.03865] [INSPIRE].

[31] A. Buckley et al., *LHAPDF6: parton density access in the LHC precision era*, *Eur. Phys. J.* **C 75** (2015) 132 [arXiv:1412.7420] [INSPIRE].

[32] A.V. Smirnov, *FIRE5: a C++ implementation of Feynman Integral REduction*, *Comput. Phys. Commun.* **189** (2015) 182 [arXiv:1408.2372] [INSPIRE].

[33] T. Gehrmann, T. Huber and D. Maître, *Two-loop quark and gluon form-factors in dimensional regularisation*, *Phys. Lett.* **B 622** (2005) 295 [hep-ph/0507061] [INSPIRE].

[34] R.K. Ellis and G. Zanderighi, *Scalar one-loop integrals for QCD*, *JHEP* **02** (2008) 002 [arXiv:0712.1851] [INSPIRE].

[35] S. Frixione, Z. Kunszt and A. Signer, *Three jet cross-sections to next-to-leading order*, *Nucl. Phys.* **B 467** (1996) 399 [hep-ph/9512328] [INSPIRE].

[36] https://www.ttp.kit.edu/preprints/2016/ttp16-051/.

[37] T. Gehrmann, L. Tancredi and E. Weihs, *Two-loop QCD helicity amplitudes for $gg \to Zg$ and $gg \to Z\gamma$*, *JHEP* **04** (2013) 101 [arXiv:1302.2630] [INSPIRE].

[38] T. Hahn, *CUBA: A Library for multidimensional numerical integration*, *Comput. Phys. Commun.* **168** (2005) 78 [hep-ph/0404043] [INSPIRE].

[39] http://www.gnu.org/software/gsl/.

JHEP01(2017)073